

A Gear Form-Grinding Optimization Method Based on Neural Network

Wenmin ZHU¹ and Zhi GENG^{2*}

0000-0002-7231-3802, 0000-0002-4513-9984

¹School of Mechanical Engineering, ShanghaiJiao Tong University, 800 Dongchuan Rd, Minhang District, Shanghai, 200240, China

²Shanghai Macrocks Technology Co., Ltd, Minhang, Shanghai, 201101, China

Abstract

Since the contact line equation is a transcendental equation, the relationship between the installation angle and the shape could not be expressed by explicit functions, which made it difficult to obtain the optimal shape, this paper firstly took three evaluation parameters of the shape, overrun, shift and offset as the objective function as well as the installation angle as variables the contact line optimization model was establish. Secondly, a neural network was introduced to solve the evaluation parameters. Through training the neural network by setting the installation angle as the input, the evaluation parameters as the output, the results show that the trained neural network can respond correctly, and has the advantages which the other method do not obtain. As an example of end relief modified helical gear, the results shows that the method can reduce the grinding errors effectively. Finally, the grinding experiments proven the effectiveness of the method.

Keywords: Gear; Gear manufacturing; Form-grinding; Optimization; Neural network

Research Article

<https://doi.org/10.30939/ijastech..1209429>

Received 02.12.2022
Revised 21.12.2023
Accepted 03.01.2023

* Corresponding author

Zhi Geng

gengzhi_vali@163.com

Address: Shanghai Macrocks Technology Co., Ltd, Minhang, Shanghai, 201101, China

Tel: +86 138-1645-4123

Fax: +86 0539 5921380

1. Introduction

To improve dynamic performance and fuel efficiency of powertrain systems, some types of automatic transmissions, i.e., automatic manual transmissions (AMTs), infinitely variable transmissions (IVTs), dual clutch transmissions (DCTs), continuously variable transmissions (CVTs), and electrically variable transmissions (EVTs), are used in automotive, maritime, and renewable energy applications [1-3]. Electric vehicles has become the main direction of automotive technology development because of its characteristics of high-energy efficiency, low emission and diversified energy source [1]. To achieve targets of high-efficiency and high-power of EVs, the integration of a high-speed motor and a gearbox is a development trend of an electric drivetrain system [2,3]. A new drivetrain scheme of a two-speed planetary gearbox and a one-way clutch can well match with the high-speed motor. A vehicle transmission transmits the rotating power of the energy source, whether an electric motor or an internal combustion engine (ICE), through a set of gears to a differential, the unit that spins the wheels [4-6]. Any vehicle, ICEs or electric vehicles, needs more torque than speed to propel the car from a dead stop, and more speed than torque once the vehicle already has forward momentum [7,8]. Comparing with traditional multi-speed gearboxes for ICEs, the two-speed gearbox is simplified but has a high requirement on its

reliability [9]. The reliability performance of the two-speed planetary gearbox of the EV is closely related to the characteristics of transmission errors of its gear pairs [10].

Cylindrical involute gears, i.e., spur and helical ones, are widely used in gearboxes and planetary gear trains in many other industrial applications [11-13]. Evolution of the design and manufacture of such gears by hobbing, shaping, and grinding has been impressive. Geometry, design and manufacture of helical gears was the subject of research represented in the works [14-16] and many others. Generally, gears are manufactured via hobbing [17,18] or forming cutting [19-21] based on the theory of gearing. For some gears with special tooth profiles, e.g., concave-convex and spiral tooth profiles, their manufacturing methods and machine-tools are complex. Since meshing performances of these gears with special tooth profiles are highly sensitive to manufacturing errors [22,23], high manufacturing accuracy of gear machine-tools is required for these gears [24-27].

Transmission errors and contact patterns are two typical methods for meshing performances evaluation of gear systems [10,28,29]. A tooth profile modeling method was developed to improve accuracy of tooth contact analysis for gear tooth profiles [30]. Some other meshing performances, e.g., power losses, can also be evaluated based tooth contact analysis [31-33]. Since these gears have convex-concave tooth profiles, they cannot be manufactured

via standard gear manufacturing methods. During a manufacture in this way, for each of the gear modules and the radius of curvature, a different blade size and gear holder is needed. However, it's clear that these gears have many advantages, if they can be produced sufficiently in the industry [34,35]. Since these gears have better load-bearing capabilities, have a balancing feature for the axial forces, quiet operation feature and their lubrication characteristics is better than herringbone gears and spur gears [36-38]. It's noteworthy that there are number of studies carried out recently in relation to these gears [39,40]. Many applications, e.g., automobile [41,42] and tunnel boring machines [43,44] require high reliability of gearboxes. Some neural network methods are also used for gear manufacturing to improve the accuracy of machine-tools [45,46].

Application of modern CNC for gear form grinding methods is introduced new concepts in design and formed of involute gears with modifications. The study describes a new reliability-enhanced form grinding method based on a predesigned second-order transmission error function. The proposed method is based on the kinematical modeling of the basic machine settings and motions of a virtual generating rack cutter. This work focus on the design of gear drives with reduced noise is based on application of a predesigned parabolic function of transmission errors.

The remaining part of this paper are organized as follows. Section 2 presents numerical model of a gear form-grinding wheel profile and its coordinate systems. Section 3 presents the proposed optimization model of the gear form-grinding wheel. Section 4 introduces the contact line between the gear form-grinding wheel and the gear. Section 5 presents an error evaluation model for gear tooth profiles. Some case studies and experimental testing are presented in Sections 6 and 7. Some conclusions from this work are presented in Section 8.

2. The Range of Form-Grinding Wheel Mounting Angle

2.1 Numerical Method of Coordinate System and Form-Grinding Wheel Profile

In order to facilitate the analysis of the study, the establishment of the coordinate system of a form-grinding wheel is shown in Fig. 1. A coordinate system $S_g(x_g, y_g, z_g)$ is established on the gear, where the z_g -axis is the gear axis. A coordinate system $S_w(x_w, y_w, z_w)$ is established on the grinding wheel, where the z_w -axis is coincident with the form-grinding wheel axis, and the a is the center distance variation of the tooth profile modification. The shortest distance between the gear axis and the form-grinding wheel axis is the center distance of a , and the angle Σ between the two axes is the angle of the form-grinding wheel.

With mold grinding helical gear, at any moment the relative motion of the gear, helical surface and grinding wheel surface tangent along the contact line contact. The contact line between the form-grinding wheel and the gear wheel is obtained by the shape of the helical gear end face and the installing parameters of the grinding wheel. The contact wire is rotated around the axis of the form-grinding wheel to obtain the profile of the form-grinding wheel. When the center distance is determined by this method, the from-

grinding wheel profile of any grinding wheel mounting angle is obtained. Determine the gear spiral surface of any obtained. Determine the gear spiral surface of any point $M(x_g, y_g, z_g)$, the grinding contact point $P(x_w, y_w, z_w)$ can be calculated on the surface of Sand loop is corresponding to the M point of helical surface of gear. The actual contact line of the form-grinding wheel and gear curve is composed of P in grinding process. The contact line can be rotated to the grinding wheel section to obtain the cross section of the form-grinding wheel, which can be represented as

$$\begin{cases} R_w = \sqrt{x_w^2 + y_w^2} \\ Z_w = z_w \end{cases} \quad (1)$$

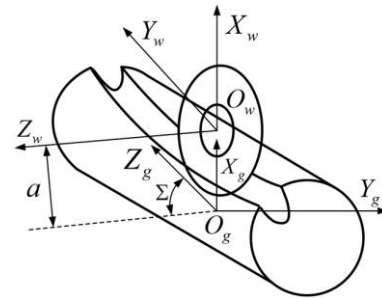


Fig. 1 Coordinate system of the form-grinding wheel

2.2 Determination of Form-Grinding Wheel Mounting Angle Range

When grinding helical gear with a forming method, the tooth root transition curve connection, the installation angle Σ of the grinding wheel Σ can be selected in a certain range, the range is based on the grinding wheel in the design of other conditions. In order to produce helical gear surface correctly, must meet the following two conditions: the contact conditions for tangency and non-interference conditions.

For the contact conditions for tangency, the installation angle of the grinding wheel selection only needs to satisfy the relation:

$$\begin{cases} a < |\Lambda| \\ |p \cot \Sigma| < |\Lambda| \end{cases} \text{ or } \begin{cases} a > |\Lambda| \\ |p \cot \Sigma| > |\Lambda| \end{cases} \quad (2)$$

where Λ is the one with the gear end section curve point coordinates of related functions, and P is the spiral parameter. For the non-interference conditions, take root transition spiral surface of any point $S_g(x_{gs}, y_{gs}, z_{gs})$ on the gear coordinate system. The point is converted to the grinding wheel coordinate system to get a point $S_w(x_{ws}, y_{ws}, z_{ws})$, The cutting radius of the form-grinding wheel at the point can be represented as

$$R_0 = \sqrt{x_{ws}^2 + y_{ws}^2} \quad (3)$$

The curvature radius of the helical gear at the point can be represented as

$$\rho = \left[1 + \left(\frac{dx_{ws}}{dy_{ws}} \right)^2 \right]^{\frac{3}{2}} / \left(\frac{d^2x_{ws}}{dy_{ws}^2} \right) \quad (4)$$

As long as $\Delta = R_0 - \rho < 0$ meet, the interference phenomenon will not occur at the S point. After determination of gear parameters and center distance, Δ is a function of Σ correlation. The range of the form-grinding wheel mounting angle can be obtained by combining the two molding conditions.

3. Optimization Model of the Form-Grinding Wheel

3.1 Geometrical Properties of the Form-Grinding Wheel

The contact line of the formed grinding helical gear is a three-dimensional curve, which is projected onto the $x_g y_g z_g$ plane of the gear coordinate system, as shown in Fig. 2. Visible contact line shape is mainly affected by the over range s_a , the offset s_b , the offset s_c three evaluation parameters. The overshoot is the length of the first point and the last point of the contact line in the z_g axis. Offset is addendum circle and circle intersection of involute tooth surface with the same length in the direction of z_g axis. The offset is the length of the dividing circle and the intersection point of the left and the right tooth surfaces in the direction of z_g axis.

For grinding, bevel gear, the contact line is in motion in the alveolar end the other end trailing traction. Therefore, the actual working stroke of the grinding wheel along the tooth width direction is the tooth width and the super range. Under certain conditions of the grinding wheel walking knife speed, the smaller the overshoot, the shorter the grinding time, the higher the grinding efficiency. Because of a tilted state contact line in cogging, about two gear tooth surface at the contact point of unbalanced force, resulting in grinding chatter. In order to reduce the unbalanced force of the wheel and the gear, the offset must be reduced. In addition, the smaller the offset is, the higher the accuracy of the modification of the additional radial moving gear teeth. When the offset tends to be the smallest, it is needed to consider the process to increase the offset and the overshoot, so the offset is only suitable for the single side grinding.

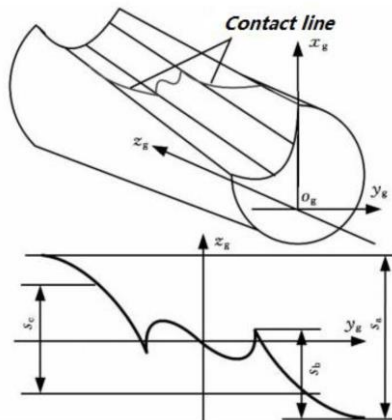


Fig. 2 Schematic diagram of the contact line between the form-grinding wheel and the gear

3.2 Analysis on Characteristics of Wheel Mounting Angle and Contact Line

From the above, to optimize the contact line in order to improve the grinding efficiency and grinding precision, must reduce the amount of overshoot, offset, offset value. The basic parameters of helical gears are shown in Table 1.

For the gear in Table 1, when the grinding wheel installation angle changes between 69 deg to 73 deg, the amount of overshoot, offset and offset of the contact line with the change of the angle of the grinding wheel is shown in Fig. 3. Along with the change of the angle of the grinding wheel, the overshoot, offset and offset are changed simultaneously, but the minimum value of the 3 quantities cannot be achieved at the same grinding wheel. For example, in Figure 3 when the overshoot, offset, offset the most hours, the grinding wheel installation angle of about 69 deg, 69.40 deg, 72.38 deg. When the angle of grinding wheel mounting angle is increased by 69.40 deg, the offset and the overshoot increase, the offset decreases and then increases. The installation angle of the grinding wheel is reduced by 69.40 deg, the offset and offset are increased, and the overshoot is reduced.

Table 1. Design parameters of the gear specimen

Item	Value
Tooth number	53
Module (mm)	5
Pressure angle (deg)	20
Helix angle (deg)	20
Coefficient of variation (mm)	0
Addendum circle diameter (mm)	292.01
Root diameter (mm)	269.51
Gear width (mm)	70
Tooth profile modification	0.02
Trimming width (mm)	10

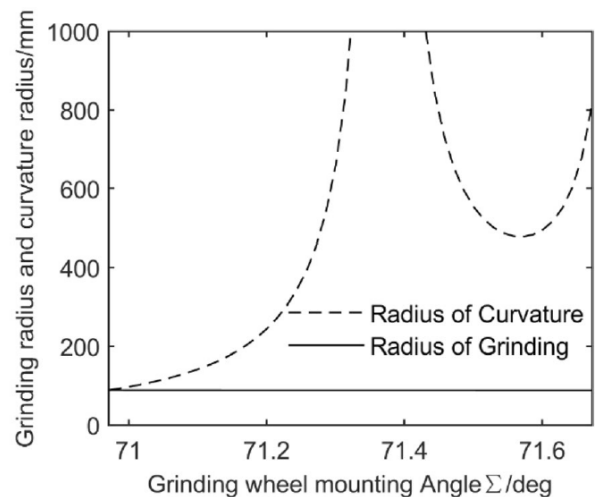


Fig. 3 Relationship between contact line and grinding wheel installation angle

3.3 Multi Objective Optimization Model of Contact Line

When optimizing the contact line, it involves a number of design targets, that is, the minimum value of the overshoot, offset and offset. At the same time, the problem of the optimal value of two or several design targets is the multi objective optimization problem. The mathematical model of the problem can be expressed as the objective function:

$$\min F = \begin{cases} \min F_1(\Sigma) \\ \min F_2(\Sigma) \\ \min F_3(\Sigma) \end{cases} \quad (5)$$

where $F_1(\Sigma)$, $F_2(\Sigma)$, and $F_3(\Sigma)$ are overrun, offset, and offset on the installation angle of the form-grinding wheel function of Σ , respectively. The constraint condition of the multi-objective optimization model of the contact line between the form-grinding wheel and the gear can be represented as

$$\Sigma_1 < \Sigma < \Sigma_2 \quad (6)$$

where (Σ_1, Σ_2) is the optional range of the mounting angle of the form-grinding wheel.

From the above, we can see that the mathematical model of the three design indicators cannot reach the best at the same time, it must be based on the actual processing needs, choose the relatively optimal solution. The theoretical basis of the constraint model is as follows: if the planning problem can be given a range of choice, the target can be excluded from the target group as a constraint. Therefore, the process needs to be selected to optimize the first target, and to the rest of the target set the range of choice. For example, when the grinding efficiency is increased, the minimum of the super range is the first target, and the offset and offset cannot exceed a range value, and the mathematical model can be rebuilt. The objective function can be represented as

$$\min F = \min F_1(\Sigma) \quad (7)$$

Constraint conditions are

$$\begin{cases} \Sigma_1 < \Sigma < \Sigma_2 \\ F_2(\Sigma) < F_2^j \\ F_3(\Sigma) < F_3^j \end{cases} \quad (8)$$

where F_2^j and F_3^j are the limit of offset and offset setting, respectively. At this point, the multi objective optimization of the amount of overshoot, offset and offset is transformed into a single objective optimization of the process.

4. Contact Line Shape Evaluation Parameter Solution

4.1 Contact Line Equation

On the solution of the contact line super range offset need to solve the contact line equation:

$$z_g n_x + a n_y \cot \Sigma + (a - x_g + p \cot \Sigma) n_z = 0 \quad (9)$$

where $\mathbf{n}(n_x, n_y, n_z)$ is the normal vector of point on spiral surface of helical gear. Equation (9) is a transcendental equation can be combined with such error algorithm and Newton iterative method for solving. The optimization is needed to solve the transcendental equation this is because the relationship between the wheel mounting angle and the overshoot, the offset and the offset cannot be expressed in a specific function with fuzziness. In order to solve this problem, we can directly fit the function between the optimization parameters and the grinding wheel mounting angle.

Based on data in Fig. 3, the straight line fitting method can be used, the advantage of this method is that the principle is simple, the disadvantage is that more manual intervention is needed and the programming is more complex. For example, the method should be based on the current gear parameters and grinding wheel installation parameters need to be fitted to several sections of straight line. It is necessary to determine the amount of overshoot, offset, offset, respectively, as the minimum value of the corresponding grinding wheel installation angle, then the fitting angle of the grinding wheel is fitted by the standard of the minimum grinding wheel. The neural network is very good at this kind of input and output relations is not explicit function approximation direct call to the neural network simulation results and not to solve the transcendental equation can shorten the calculation time and reduce the artificial intervention. Among all kinds of neural networks, BP neural network is the most widely used, and the basic function of BP neural network is function approximation.

4.2 Evaluation Parameter Solving Model

Let $(\Sigma^{(k)}, F_1^{(k)}, F_2^{(k)}, F_3^{(k)})$, where $k=1,2,\dots,n$, are input output sample pair grinding wheel mounting angle input data, among $\Sigma^{(k)} = [\Sigma_1 \ \Sigma_2 \ \dots \ \Sigma_n]^T$ are grinding wheel mounting angle input data $F_m^{(k)} = [f_1^{(m)} \ f_2^{(m)} \ \dots \ f_n^{(m)}]$ are output data for overshoot, offset and offset. Σ as the input of the network, in the role of continuous power, the actual output of the network can be $Y_m^{(k)} = [y_1^{(m)} \ y_2^{(m)} \ \dots \ y_n^{(m)}]^T$. The connection weights of i to j are w_{ij} , and the weights of the weights are Δw_{ij} and the mean square error of the model can be represented as

$$\Delta w_{ij} = \eta \delta_j v_i \quad (10)$$

$$e_m = \frac{1}{n} \sum_{k=1}^n K(f_k^{(m)} - y_k^{(m)})^2 \quad (11)$$

After a lot of trial calculation, the function approximation ability has little relation with the number of hidden layer, so the BP neural network with single hidden layer is adopted in this problem. This point is consistent with the reference [10], the transfer function of hidden layer neurons with S tangent function, the output layer transfer function of neurons with S logarithmic function. At 69.32

deg ~ 71.53 deg, the value of the 200 grinding wheel mounting angle is calculated, and the corresponding super range, offset and offset are calculated as training samples. According to the above method, the neural network model is established with the training parameters shown in Table 2. The training results of the model are shown in Figure 4, after 15 iterations, when the mean square error converges to 8.32456×10^{-6} , the network performance can meet the requirements of the target.

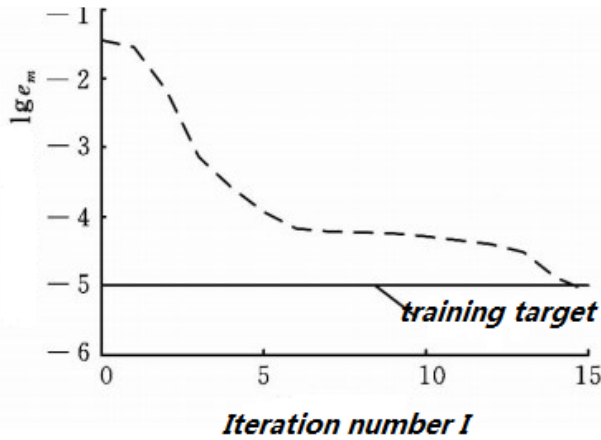


Fig. 4 Neural network modeling training results

The calculation error curve between the values shown in Fig. 5 the true value for the offset and the neural network shows that network computing is very small value between real value and error, except in the vicinity of 69.32 deg ~ 69.4 deg appeared relatively large error, the error is relatively small. Causes the larger relative error in the area can be reflected in Fig. 3, as close to the minimum value of the offset and offset minimum at a value for mutation, so use neural network to calculate, will make a larger relative error, but even offset and real value at the maximum error also the deviation is only 0.2 mm.

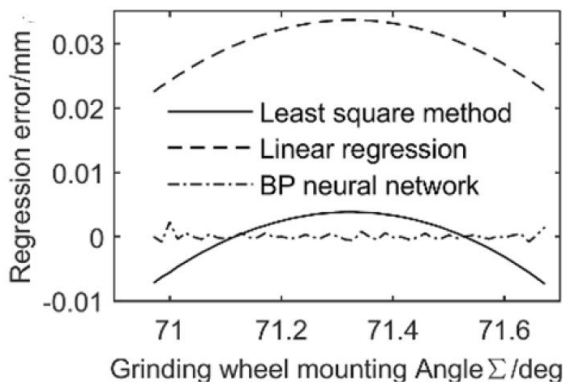


Fig. 5 Offset error curve

Observation Figs. 6 and 7 found that the error of the overshoot and offset is very small, this is because the grinding wheel in the training sample installation angle range of the range of the overshoot and the bias is monotonous, there is no point mutation.

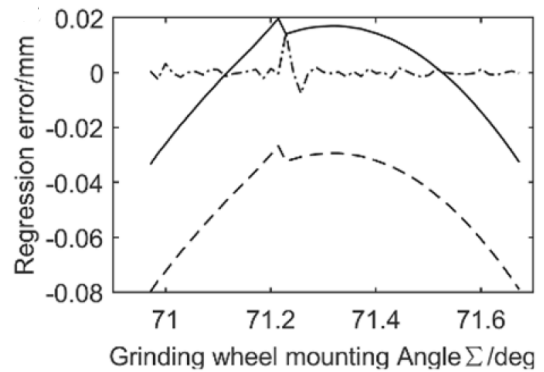


Fig. 6 Overshoot error curve

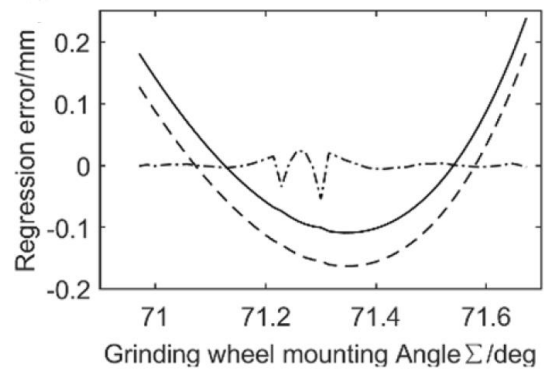


Fig. 7 Offset error curve

5. Error Analysis Model

In order to verify the contact line optimization effect, need to reverse the calculation, which is the best installation angle of the grinding wheel to calculate grinding wheel, grinding wheel was calculated according to the grinding tooth surface, so that with the tooth surface design, solving the grinding error.

Three additional motions can be selected in the tooth profile modification of the gear, the variation of center distance, the rotation of the gear wheel and the axial movement of the grinding wheel. There is no requirement for the gear in the gear shape modification, so as to facilitate the establishment of error analysis model, this paper establishes the error analysis model by taking the angle of the bevel gear and the grinding wheel as an example.

If the grinding wheel inverse to tooth surface point of $T(x_T, y_T, z_T)$, and a little on the point corresponding to the design of spiral gear surface is $Q(x_Q, y_Q, z_Q)$, the design of grinding error of spiral surface and the actual machining helical surface:

$$e = \sqrt{(x_0 - x_T)^2 + (y_0 - y_T)^2 + (z_0 - z_T)^2} \tag{12}$$

6. Case study

For the convenience of calculation of gear grinding errors, select only the requirements of modified helical gear tooth (Table 1) as

an example, in addition, because the grinding experiment is used to process the one side grinding respectively around the tooth surface, so the calculation results as a precondition for optimization.

6.1 Evaluation Parameter Analysis

In order to meet the conditions of non-interference in the grinding wheel and the gear, helical gear should be greater than the radius of curvature of the grinding wheel cutting radius, by using the calculation method of section first wheel angle can be calculated, the installation angle of the grinding wheel is in the range of 69.32 deg ~ 71.53 deg, as shown in Fig. 8, after calculation, the range of full contact conditions.

After determining the scope of the grinding wheel installation angle, set the value of the wheel installation angle and draw the corresponding curve of the contact line, as shown in Fig. 9. When the wheel angle of 70 deg (sigma complementary and helix angle) angle), the offset is 4.11 mm, overrun is 9.98 mm, offset is 7.12 mm; when the installation angle of the grinding wheel $\Sigma = 71.2528$ deg (complementary and base helix angle), offset length is 13.47 mm, super capacity was 6.82 mm, offset is 3.84 mm; when the installation angle of the grinding wheel is 69.40 deg, the offset is 0.16 mm, super capacity is 6.67 mm, and the offset is 8.4 mm.

As can be seen from the above, three evaluation parameters in the same installation angle of the grinding wheel, some for some small value to a large value, so we should choose the installation angle of the grinding wheel, must be considered to overrun, offset, offset. In the actual grinding, axial modification in order to reduce the grinding error, should offset the reduction of contact line, at the same time when one side grinding bias and super volume should not be too large, therefore, the contact wire in multi-objective optimization, the minimum offset for the first goal, to offset and overrun value constraint.

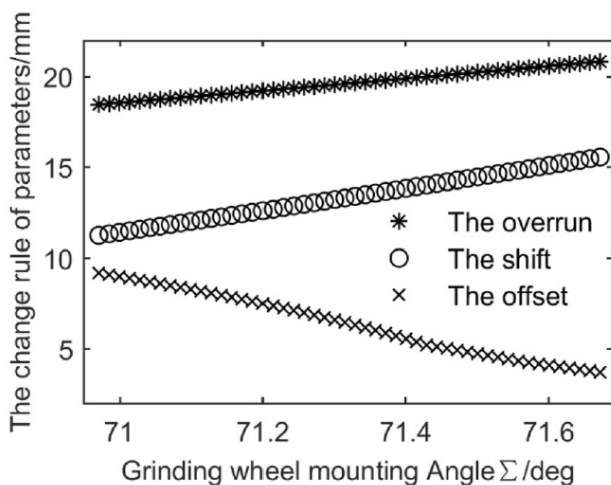


Fig. 8 Grinding wheel mounting angle range under the condition of non-interference

Optimization method according to the second section and the third section after the installation angle of the grinding wheel

$\Sigma = 69.80$ deg, the offset is 2.68 mm, overrun is 8.80 mm, offset is 4.22 mm. In addition, in the actual machining and installation angle of the grinding wheel is complementary with the base helix angle, i.e., $\Sigma = 71.2528$ deg, compared with the installation angle of the grinding wheel grinding wheel with $\Sigma = 71.2528$ deg, the optimized installation angle, offset decreases about 80.1%, overrun decreased by about 47.7%, offset increases about 9.9%. The offset and overrun decreased, but the bias increases, but increases only 0.38mm. Comprehensive consideration, the contact line shape of the grinding wheel installation angle of 69.80 deg is better than that of the contact line when the grinding wheel installation angle is 71.2528 deg.

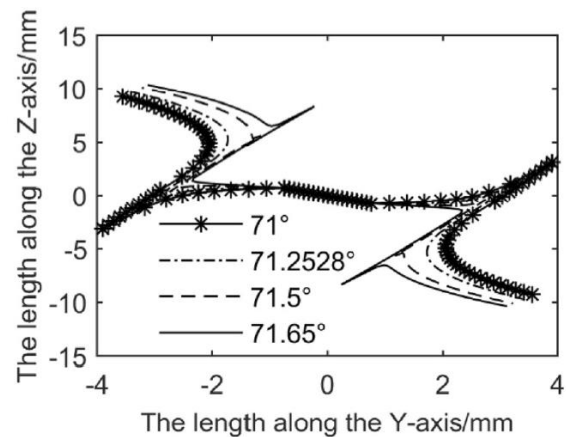


Fig. 9 Comparison of different grinding wheel mounting angle contact lines

6.2 Grinding Error Analysis

This section is mainly on the grinding wheel installation angle of 71.2528 deg and 69.80 deg when the gear grinding error analysis and comparison. To evaluate the tooth to tooth surface error, first calculate the different axial positions of the theoretical tooth surface, and the fourth section grinding wheel tooth surface is compared against the tooth surface will start in the meshing line, tooth width as the horizontal axis, the tooth surface expansion length for the vertical axis, launched by the length of exhibition angle to say get Fig. 10, top gear at the top, at the bottom of the root.

Figure 10(a) is a distribution map of the installation angle of the grinding wheel $\Sigma = 71.2528$ deg tooth surface error, in the middle part of the tooth width without modification part. Figure 10(b) is a distribution map of the installation angle of the grinding wheel $\Sigma = 69.80$ deg tooth surface error.

By comparing Figs. 10(a) and 10(b) can be found, the additional radial motion of straight tooth end tooth modification, distribution of symmetrical tooth surface error on gear tooth width on both sides of the symmetrical surface error, and the top of the teeth than the tooth root of tooth surface error. After optimization, the maximum tooth surface error is reduced from 8 um to 5 um, and the optimum grinding wheel mounting angle can obviously reduce the maximum tooth surface error.

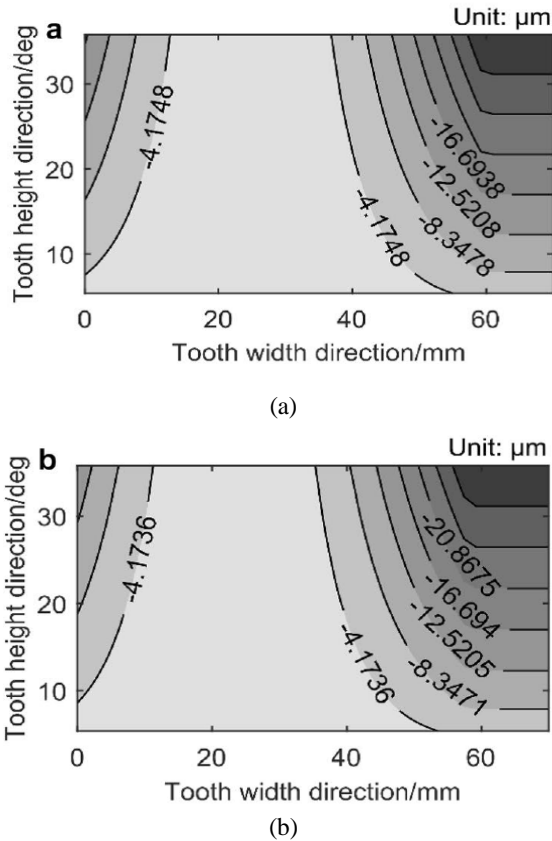


Fig.10 Grinding error of grinding tooth surface

The result of error analysis shows that the machining error distribution is more uniform and the accuracy is higher than that before the optimization of the contact line, which can meet the requirements of the practical engineering application.

7. Grinding Gear Machining Experiment

In this paper, the grinding gear processing experiments using self developed multi function forming grinding machine, machining gear and machine tools as shown in Fig. 11. In Table 2, the helical gear parameters, combined with the actual processing requirements of the contact line optimization calculation to determine the installation angle of the grinding wheel grinding wheel, grinding and programming in NC machining finish grinding wheel dressing and automatic gear.

In order to compare the precision grinding, to eliminate the effect caused by different gear blanks, using the same gear unilateral grinding manner in the machining process, the left and right flanks respectively to the installation angle of the grinding wheel $\Sigma = 71.2528$ deg and $\Sigma = 69.80$ deg grinding wheel and calculation of gear grinding and other parameters of two tooth surface processing consistent. In order to compare the grinding efficiency, the time of grinding tooth surface is recorded.

After finishing grinding experiment, the gear measuring instrument which is produced by Harbin Precision Instrument Co., Ltd. is tested, as shown in Fig. 12.

Table 2 Machine-tool settings of form-grinding tests

Parameters	Values
Spindle speed (rad/min)	4200
Grinding linear velocity (m/s)	35
Feed velocity (m/s)	0.02



Fig. 11 Helical gear grinding experiment



Fig. 12 Gear tooth surface measurement

The tooth test report as shown in Fig. 13, the processed gear has reached the national standard of 3 grade precision, compared to about two teeth, the tooth surface precision is obviously higher than that of the left and right flank, visible after the optimization, the accuracy has been greatly improved, this is mainly because the offset after the optimization of the contact line decreases, the grinding vibration obtained the relief.

The tooth to the test report as shown in Fig. 14, after processing the gear precision reach grade 5 according to national standards, the right tooth modification effect is very good, to achieve 3 GB, the left tooth surface in the processing of the offset and offset due to the contact line is too large to produce the "modification distortion", so it only reaches the five level.

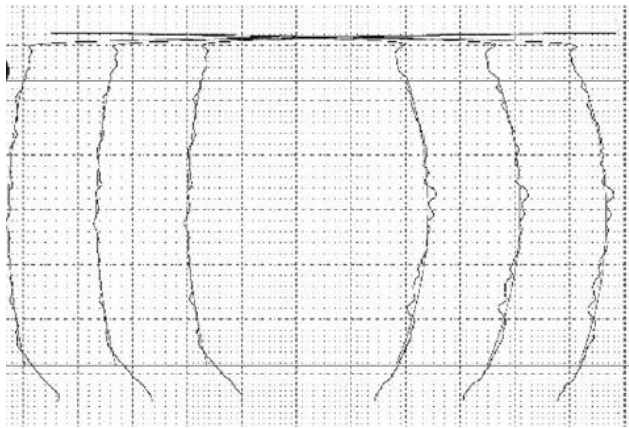


Fig. 13 Tooth profile test report

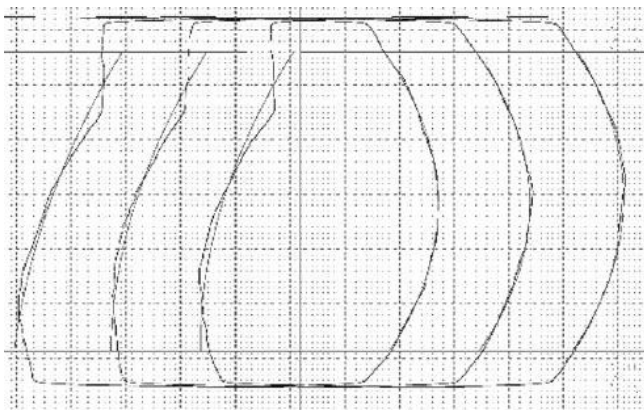


Fig. 14 Teeth inspection report

Overrun the left line of contact process is greater than the right tooth surface overrun, so the left tooth surface grinding needs a longer period of time, in the process under the same conditions, complete left tooth surface processing takes about 32 min, right flank takes about 27 min, visible in mass production, the optimized installation angle of the grinding wheel can effectively improve grinding efficiency.

8. Conclusions

Theoretically, the proposed form grinding method for cylindrical involute gears based on the optimization of the form-grinding wheel is not limited to the involute tooth profile, and is applicable to all types of gears. Because of the light load cases can reflect more gear noise problems. Especially, involute gears with time-varying meshing stiffness are difficult to adjust amount of modification. Therefore, on the basis of the obtained results, the following conclusions can be made:

(1) The grinding wheel and the helical gear grinding motion is studied, based on analytic formula of grinding wheel, wheel design conditions determined without interference wheel angle range.

(2) Study on the properties of the contact line, analyzed the three parameters influence on the contact line, the optimization model

was established based on the method of contact line constraint, in solving the evaluation parameters, to solve the contact line conditions using neural network.

(3) An error analysis model is established for the modification of the linear tooth end of the additional radial motion. The validity of the method is verified by the calculation examples and the grinding tooth experiment.

(4) Comprehensive consideration, the contact line shape of the grinding wheel installation angle of 69.80 deg is better than that of the contact line when the grinding wheel installation angle is 71.2528 deg. After optimization, the maximum tooth surface error is reduced from 8 μm to 5 μm , and the optimum grinding wheel mounting angle can obviously reduce the maximum tooth surface error.

Acknowledgment

The author is grateful for the financial support from the Shanghai Education Commission, Science and Technology Innovation Projects, Grant No. 11CXY45.

Conflict of Interest Statement

There is no conflict of interest in the study.

CRedit Author Statement

Wenmin Zhu: Conceptualization, Writing-original draft, Data curation, Software.

Zhi Geng: Conceptualization, Supervision, Writing-review&editing, Validation,

References

- [1] Chen LL, Zhang H, Ni F. Present situation and development trend for construction of electric vehicle energy supply infrastructure. *Power Syst Technol.* 2011;35(14):11–17.
- [2] Geng Z, Li G. Optimal clutch control of a one-way clutch assistant transmission for electrical vehicles. *Int J Auto Sci Tech.* 2022;6(3):257-264.
- [3] Lu TL, Dai F, Zhang JW, Wu MX. Optimal control of dry clutch engagement based on the driver's starting intentions. *Proc Instn Mech Eng, Part D: J Automob Eng.* 2012;226(8):1048-1057.
- [4] Di X, Huang Y, Ge Y, Li G, Hu M. Fuzzy-PID speed control of diesel engine based on load estimation. *SAE Int J Engines.* 2015;8(4):1669-1677.
- [5] Huang Y, Wan G, Cui T, Li G. A study on engine control strategy for gear shifting of AMT. *Automotive Engineering.* 2012;34(3):245-248.
- [6] Jiang D, Huang Y, Li G, Hao D, Zuo Z. Design of a speed tracking controller for heavy-duty vehicles with an all-speed governor based on a model predictive control strategy. *Int J Engine Res.* 2017;18(9):930-940.
- [7] Li G, Zhu WD. Experimental investigation on control of an infinitely variable transmission system for tidal current energy converters.

- IEEE/ASME Trans Mechatron. 2021; 26(4):1960-1967.
- [8] Li G, Zhu WD. Theoretical and experimental investigation on an integral time-delay feedback control combined with a closed-loop control for an infinitely variable transmission system. *Mech Mach Theory*. 2021;164:104410.
- [9] Li X, Li G, Ren J, Li W. Numerical simulation of helical gear tooth root crack initiation life of high-speed EMUs. *China Mech Eng*. 2018;29(09):1017-1024.
- [10] Wang ZH, Wang J, Wang QL, Li G. Transmission error of spiral bevel gear based on finite element method. *J of Vib Shock*. 2014;33(14):165-170.
- [11] Hu YH, Li G, Zhu WD, Cui JK. An elastic transmission error compensation method for rotary vector speed reducers based on error sensitivity analysis. *Appl Sci*. 2020;10(2):481.
- [12] Yan J, Li G, Liu K. Development trend of wind power technology. *Int J Adv Eng Res Sci*. 2020;7(6):124-132.
- [13] Li G, Zhu WD. Time-delay closed-loop control of an infinitely variable transmission system for tidal current energy converters. *Renew Energy*. 2022;189:1120-1132.
- [14] Li G. Design and modeling of an impulse continuously variable transmission with a rotational swashplate. *Int J Auto Sci Tech*. 2020;4(4):307-313.
- [15] Xu M, Zhang X, Hu G, Li G. The structure design and flow field simulation of a fire water monitor driven by worm gear with bevel gear. *Mach Tool & Hydra*. 2016;6:57-61.
- [16] Gu KL, Wang ZH, Li G, Liu XR. Optimization of geometric parameters of the straight conjugate internal gear pump based on GA. *Elec Sci Tech*, 2017;30(6):39-42.
- [17] Zhang XL, Wang ZH, Li G. Research on virtual hobbing simulation and study of tooth surface accuracy of involute helical gears. *Appl Mech Mater*. 2012;155:601-605.
- [18] Wang ZH, Li G, Zhang XL, Li KS. Study on the virtual hobbing simulation and tooth surface accuracy of the entirety of involute helical gears. *J Mech Trans*. 2012;36(8): 9-13.
- [19] Li G, Wang ZH, Zhu WD, Kubo A. A function-oriented active form-grinding method for cylindrical gears based on error sensitivity. *Int J Adv Manuf Tech*. 2017;92(5-8):3019-3031.
- [20] Wang ZH, Zhu WM, Li G, Geng Z. Optimization of contact line for form-grinding modified helical gears based on neural network. *China Mech Eng*. 2014;25(12):1665-1671.
- [21] Li G. An active forming grinding method for cylindrical involute gears based on a second-order transmission error model. *SCIREA J Mech Eng*. 2019;2(1):1-14.
- [22] Li G, Zhu WD. An active ease-off topography modification approach for hypoid pinions based on a modified error sensitivity analysis method. *ASME J Mech Des*. 2019;141(9):093302.
- [23] Li G, Wang ZH, Kubo A. Error-sensitivity analysis for hypoid gears using a real tooth surface contact model. *Proc Instn Mech Eng, Part C: J Mech Eng Sci*. 2017;231(3):507-521.
- [24] Zhang WX, Wang ZH, Liu XR, Li G, Wan PL, Wang W. Research on optimization of temperature measuring point and thermal error prediction method of CNC machine tools. *J Shaanxi University of Tech (Na Sci Ed)*. 2017; 33(3):18-24.
- [25] Wang ZH, Cao H, Li G, Liu XR. Compensation of the radial error of measuring head based on forming grinding machine. *J Mech Trans*. 2017;41(3):143-146.
- [26] Wang ZH, Song XM, He WM, Li G, Zhu WM, Geng Z. Tooth surface model construction and error evaluation for tooth-trace modification of helical gear by form grinding. *China Mech Eng*. 2015;26(21):2841-2847.
- [27] Li G, Wang ZH, Kubo A. Tooth contact analysis of spiral bevel gears based on digital real tooth surfaces. *Chin J Mech Eng*. 2014;50(15):1-11.
- [28] Wang ZH, Wang J, Ma PC, Li G. Dynamic transmission error analysis of spiral bevel gears with actual tooth surfaces. *J Vib Shock*. 2014;33(15):138-143.
- [29] Geng Z, Li G. A reliability-enhanced forming grinding method of cylindrical involute gears for electrical vehicles. *Int J Auto Sci Tech*. 2022;6(4):317-323.
- [30] Li G, Wang ZH, Kubo A. The modeling approach of digital real tooth surfaces of hypoid gears based on non-geometric-feature segmentation and interpolation algorithm. *Int J Prec Eng Manuf*. 2016;17(3):281-292.
- [31] Li G, Zhu WD. Design and power loss evaluation of a noncircular gear pair for an infinitely variable transmission. *Mech Mach Theory*. 2021;156:104137.
- [32] Wei XT, Zhu JP, Li G. Automatic NC Programming for chamfering addendum of spiral bevel gear based on UG/Open. *Appl Mech Mater*. 2013;365:950-954
- [33] Li G, Geng Z. Gear bending stress analysis of automatic transmissions with different fillet curves. *Int J Auto Sci Tech*. 2021;5(2):99-105.
- [34] Huang DQ, Wang ZH, Li G, Zhu WD. Conjugate approach for hypoid gears frictional loss comparison between different roughness patterns under mixed elasto-hydrodynamic lubrication regime. *Tribol Int*. 2019;140:105884.
- [35] Li G, Wang ZH, Zhu WD. Prediction of surface wear of involute gears based on a modified fractal method. *ASME J Tribol*. 2019;141(3):031603.
- [36] Wu J, Wang ZH, Li G. Study on crack propagation characteristics and remaining life of helical gear. *J Mech Trans*. 2014;38(12):1-4.
- [37] Li G, Wang ZH, Geng Z, Zhu WM. Modeling approach of digital real tooth surfaces of hypoid gears based on non-geometric-feature segmentation and interpolation algorithm. *Chin J Mech Eng*. 2015;51(7):77-84.
- [38] Li G, Geng Z. Tooth contact analysis of herringbone rack gears of an impulse continuously variable transmission. *Int J Auto Sci Tech*. 2021;5(1):52-57.
- [39] Wang ZH, Yuan KK, Li G. Optimization identification for dynamic characteristics parameters of sliding joints based on response surface methodology. *China Mech Eng*. 2016;27(5):622-626.
- [40] Hu YH, Li G, Hu AM. Iterative optimization of orbital dynamics based on model prediction. *Front Arti Intel App*. 2019;320:76-86.
- [41] Wan GQ, Huang Y, Zhang FJ, Li G. Integrated powertrain control for gear shifting. *Appl Mech Mater*. 2012;148: 725-730.
- [42] Zhou Y, Huang Z, Zhang F, Jing S, Chen Z, Ma Y, Li G, Ren H. Experimental study of WC-Co cemented carbide air impact rotary drill teeth based on failure analysis. *Eng Fail Anal*. 2013; 36, 186-198.

- [43]Li G, Chen YD, Wang B, Wang WS. Dynamics simulation of a six-DOF tunnel segment erector for tunnel boring machine based on virtual prototype. *Appl Mech Mater.* 2013; 251, 231-234.
- [44]Li G, Wang B, Chen YD, Wang WS. Numerical simulation of the rock fragmentation process induced by TBM cutters. *Appl Mech Mater.* 2013; 249, 1069-1072.
- [45]Fang C, Ge H, Wang R. Effect of grinding wheel eccentricity on unilateral gear form grinding profile error. *Computer Integrated Manufacturing Systems*, 2012; 18(11), 2509-2514.
- [46]Noriteru N, Youichi K, Yasuhiko O. Tooth flank modification processing of helical gears by form grinding. *Mechanical Engineers.* 1999, 65(639), 4458-4463.